FULL PAPER

Experimental study of a new furan-2-ylmethylene-hydrazide as a corrosion inhibitor in acidic media

Nbras Hussein Ali[a],* |**Israa M.H. Almousawi[b]** |**Intisar Yahiya Mohammed[a]**

[a]*Directorate of Materials Research, Ministry of Science and Technology, Baghdad, Iraq*

[b]*Department of Chemistry, College of Science, University of Baghdad, Baghdad, Iraq*

***Corresponding Authors:**
Nbras Hussein Ali
Email: nbrasali72@gmail.com
Tel.: +009647716005755

Newly synthesized Furan-2-ylmethylsulfanyl-acetic acid (N-thiobenzoyl)-Hydrazide (FATH) was studied as Corrosion inhibitor for carbon steel (CS) in hydrochloric acid solution using potentiodynamic polarization. FATH is a good carbon steel inhibitor in 0.1 M HCl solution, according to the experimental results. With increasing inhibitor concentrations, the inhibition efficiency improved, reaching 99.9% at 600 ppm. Thermodynamic parameters for inhibitor adsorption on carbon steel were calculated and discussed. The inhibitors adsorption on the carbon steel surface followed the Langmuir adsorption isotherms.

KEYWORDS

Corrosion inhibitor; potentiodynamic polarization; Langmuir adsorption isotherms.

Introduction

Corrosion is a phenomenon that cannot be avoided. Corrosion is a chemical or electrochemical reaction that occurs when a material, usually a metal, reacts with its surroundings that causes the materials and their properties to deteriorate. Metal corrosion resistance is a significant industrial and scientific issue. Several methods have been developed and implemented to protect metals from corrosion. The most common of these strategies is the use of corrosion inhibitors [1,2]. Corrosion inhibitors are chemicals that prevent corrosion when they are adsorbed onto the metal-solution interface *via* physisorption or chemical adsorption. Several heterocyclic molecules in the aromatic or long chain carbon system combining nitrogen, oxygen, and Sulphur have been proved as effective inhibitors [3-5].

The aim of this research was to investigate whether the newly synthesized Furan-2-ylmethylsulfanyl-acetic acid (N-thiobenzoyl)-Hydrazide ($C_{14}H_{15}N_3S_2O_2$) [6] could prevent carbon steel from corroding in 0.1 M hydrochloric acid solution, as shown in Figure 1. The effectiveness of inhibition was assessed using potentiodynamic polarization.
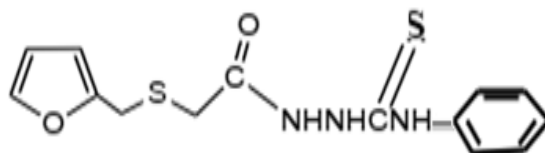
FIGURE 1 Chemical structure of furan-2-ylmethylene-hydrazide (FATH)

Eurasian Chemical Communications

Experimental method

Preparation of carbon steel samples

The metallic elements in carbon steel sheet (A106) are presented in Table 1 as a percentage of the total content. Mechanical press cutting of carbon steel into square specimens with a diameter of 2 cm and a thickness of 2 mm was used. The specimens were polished with emery sheets ranging from 80 to 2000 grit, washed in distilled water, degreased in acetone, and dried at room temperature.

TABLE 1 Chemical composition for carbon steel

Grade	% C	%Cu	% Si	% Mn	%S	%V	% P	% Ni	% Cr	%Mo	%Fe
A106	0.30	0.40	0.10	0.29-1.26	0.035	0.08	0.035	0.40	0.40	0.15	96.84-97.81

Blank solution

The corrosive test environment consisted of 10 mL of dilute concentrations of 0.1 HCl acid medium made with analytical grade HCl acid (37 percent) and distilled water.

Inhibitor solution

Three concentrations of inhibitor (FATH) (400 ppm, 500 ppm, and 600 ppm) were made by dissolving 0.004, 0.005, and 0.006 gm in 10 mL absolute ethanol, respectively, and then transferring each to a 500 mL volumetric flask containing 2.18 mL of 0.1 M HCl previously dissolved in distilled water.

Electrochemical measurements

Electrochemical studies were performed using a 500 mL Pyrex corrosion cell with three electrodes, as illustrated in Figure 2. For the electrochemical measurements, a three-electrode compartment cell was used. The reference electrodes were a saturated calomel electrode (SCE) and a platinum electrode, while the counter electrode was carbon steel specimens. The voltage across the open circuit was measured. The potential was recorded, and the polarization curve was started from the open circuit at a scan rate of 2.0 mV s^{-1} over a potential range of (+200 to -200 mV). The I_{corr} and E_{corr} were both calculated. The output was plotted for the blank solution, as well as with the addition of varied inhibitor doses. Figure 3 illustrates the complete system for polarization measurements.
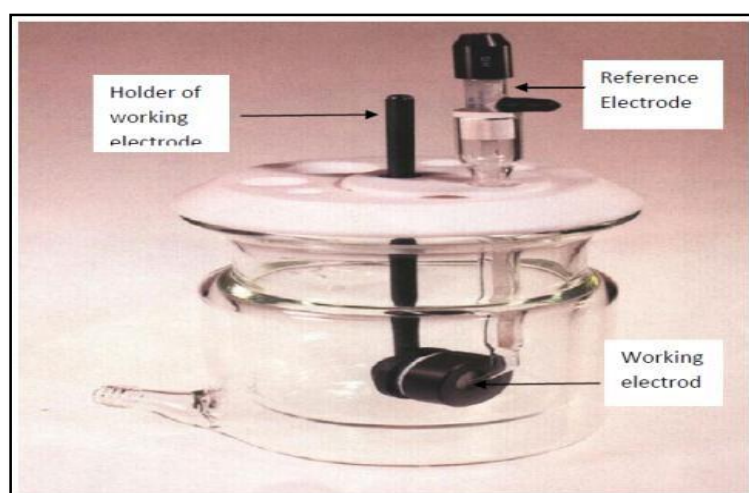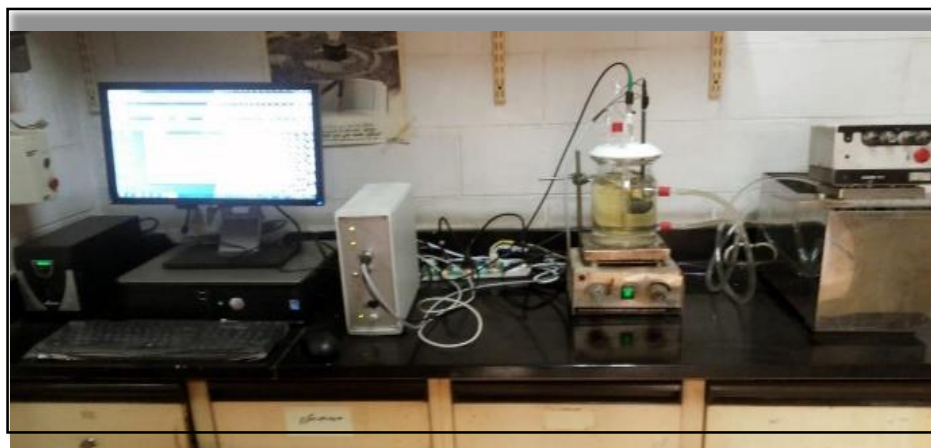

FIGURE 2 Corrosion cell

FIGURE 3 Complete system for polarization measurements

Result and discussion

Polarization measurements were used to learn more about the kinetics of anodic and cathodic reactions. The polarization is represented by Figure 4 for CS electrode curves in 0.1 M HCl solution with and without varied quantities of additives inhibitor. I_{corr} (corrosion current density), E_{corr} (corrosion potential), CR (corrosion rates), b_a (anodic Tafel slope), and b_c (cathodic Tafel slope), are electrochemical kinetic characteristics. They are derived using the extrapolation approach, and are shown in Table 2 with temperatures ranging from 298 to 328 K. The protection efficiency (%PE) was calculated using polarization data and the formula below (Equation 1) [7].

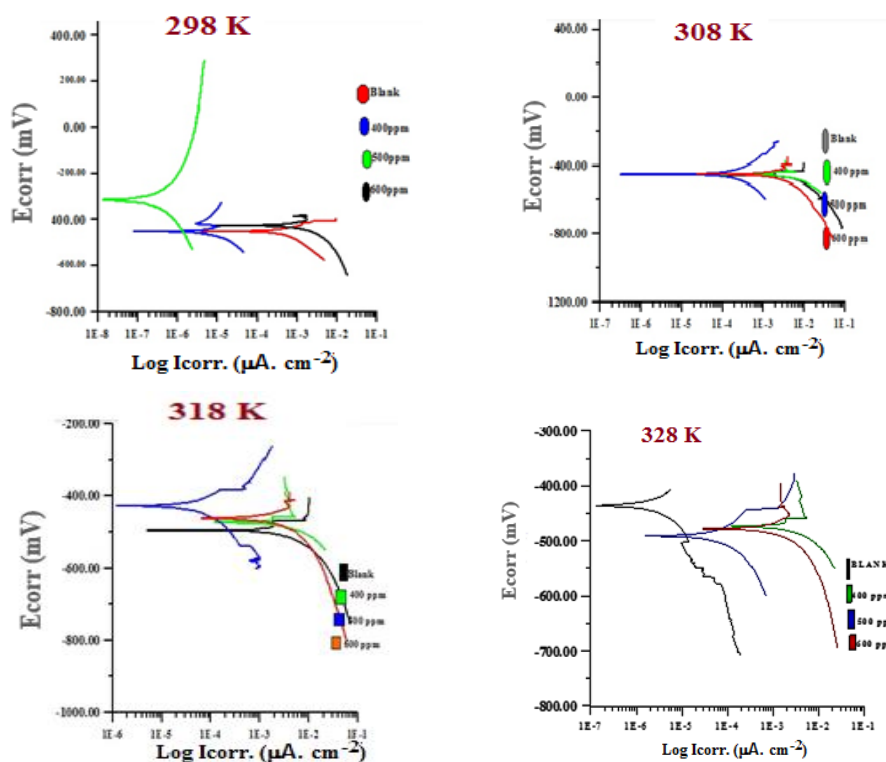$$\% \, PE = \frac{(i_{corr}) - (i_{corr})inh}{(i_{corr})o} * 100 \tag{1}$$

FIGURE 4 Tafel curves for CS in 0.1 M HCl solution with and without varied quantities of additives inhibitor FATH at different temperatures

TABLE 2 Corrosions parameter for carbon steel in 0.1 M hydrochloric acid solution with and without varied concentration of FATH inhibitor.

Conc. (ppm)	Temp. (K)	Ecorr (mv)	Icorr (µA/cm2)	ba (mv/dec)	bc (mv/dec)	CR (g/m2. y)	PE%	θ
Blank		452.615	150.6	28.822	29.471	16.67		
400	298	450.766	34.4	38.214	52.729	0.038	77.4	0.774
500		486.673	15.45	286.037	361.648	17.09	90	0.90
600		314.773	0.1145	67.637	82.660	0.12	99.9	0.999
Blank		-470.516	196.1	495.961	588.718	21.69		
400	308	-453.794	91.4	29.958	34.593	10.11	53	0.53
500		-509.129	20.4	0.771	387.727	22.58	89	0.89
600		-451.608	36.37	26.267	29.048	0.40	81.4	0.814
Blank		-498.667	2367	25.923	59.906	26.19		
400	318	-473.275	1175	27.767	26.597	13	50.3	0.503
500		-712.743	907	533.211	199.706	10.04	62	0.62
600		-426.480	39.55	76.614	78.306	0.43	98.3	0.983
Blank		-435.942	2483	75.327	58.970	27.48		
400	328	-489.476	1070	38.851	24.503	11.89	57	0.57
500		-461.284	1480	131.439	121.607	16.38	40	0.40
600		-492.230	40.76	31.173	40.152	0.45	98.3	0.983

The corrosion current densities for carbon steel electrodes in the absence and presence of inhibitor are i(corr) and i(corr)$_{inh}$, respectively. By increasing inhibitor concentrations, the corrosion current densities drop and inhibition efficiency PE% increases, as shown in Table 2.

The diminishing inhibition performance as the temperature of the solution rises could be attributed to an increase in the mobility of the inhibitor molecules, which leads to a decrease in the contact between the inhibitor molecules and the carbon steel surface [8-10]. The inhibitory efficacy of FATH was lowered at a higher temperature solution, implying that FATH molecules on metallic surfaces are adsorbing by physical adsorption [11,12], also inhibitor molecule adsorption on the steel surface is facilitated by the presence of heteroatoms (S, O, N) and multiple € bonds in their molecule [13,14].

As shown below, the activation energy (E_a) was computed using the Arrhenius equation (Equation 2) [15,16].

$$Log\ i_{corr} = log\ log\ A + \frac{E_a}{2303\ T} \qquad (2)$$

Where A is the pre-exponential factor of Arrhenius, T is the absolute temperature, and R is the gas constant. Table 3 shows the activation energies in the absence and presence of inhibitor FATH based on the slope values of Arrhenius plots (Figure 5).
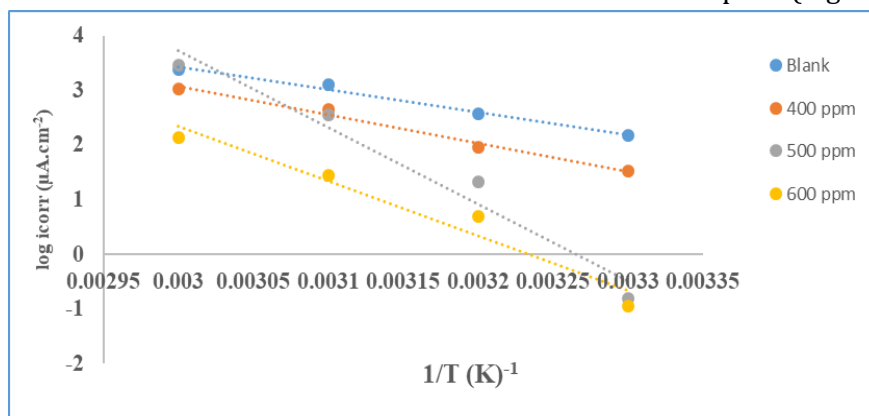

FIGURE 5 Arrhenius plots for CS in 0.1 M HCl solution with and without varied quantities of additives inhibitor FATH at different temperatures

TABLE 3 Activation parameters of carbon steel corrosion in the absence and presence of FATH in 0.1 M HCl

Conc. of FATH ppm	E_a (kJ/mol)	A (Molecule/ cm² S)	R^2
Blank	80.417	9.659 E+24	0.987
400	99.565	1.124 E+25	0.986
500	268.825	2.761 E+25	0.982
600	191.854	1.951 E+25	0.951

As in Figure 5, a straight line (R^2>0.95) for the Arrhenius plots was confirmed by the validity approach. Because the FATH molecule forms a protective coating at metal-electrolyte interfaces, the activation energies in the presence of the inhibitor are higher than in the absence of the inhibitor, indicating that a higher energy barrier has been reached and the corrosion process has become more difficult [9].

Adsorption isotherm

Understanding the adsorption mechanism of organic molecules on a metallic surface requires a thorough understanding of the adsorption isotherm. The adsorption isotherm study gives structural and thermodynamic information on the electric mono layer. In order to get the isotherm displayed below, the degree of surface covering for the various inhibitor concentrations was estimated (Equation 3).

$$\theta = \frac{PE\ PE}{100\ 100} \quad (3)$$

For FATH compound, various adsorption isotherms such as Freundlich and Langmuir adsorption isotherms were examined, and Langmuir adsorption isotherm fitted the experimental data the best. The relationship of Langmuir isotherm is defined in Equation 4 [17]:

$$\frac{C}{\theta} = \frac{1}{K_{ads}} + C \quad (4)$$

Where θ is the degree of surface covering, C is the mg/L concentration in the bulk of the solution, and K_{ads} is the adsorption equilibrium constant. The plots of C/θ vs C (Figure 6) show straight lines with a slope equal to $1/K_{ads}$ in this case. The adsorption power or binding strength of the FATH compound on the carbon steel surface is represented by the K_{ads} value. The K_{ads} values are displayed in Table 4.
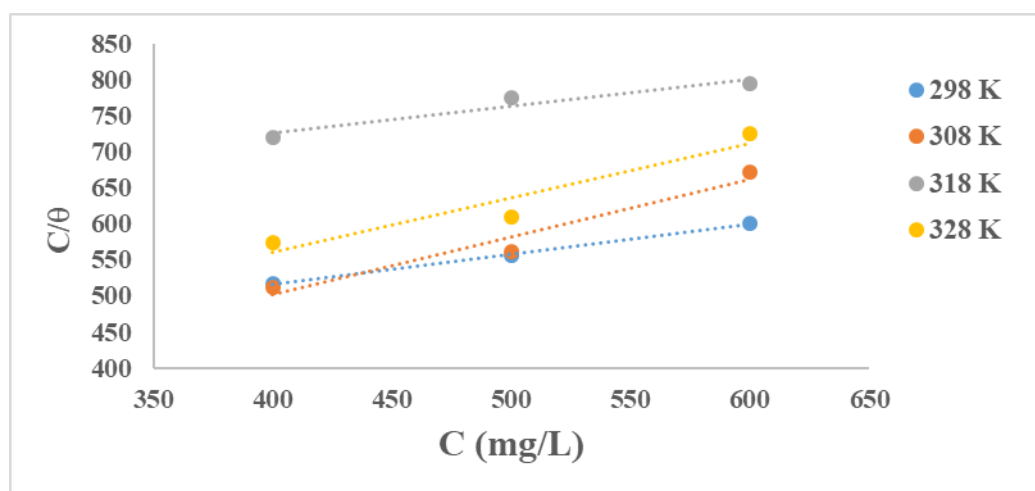

FIGURE 6 Langmuir adsorption isotherm plots for the adsorption of FATH compound on carbon steel surface at different temperatures

TABLE 4 Langmuir adsorption isotherm data

| Temp. (K)	$K_{ads.}$ (L mol^{-1})	R^2
298	924.698	0.998
308	651.625	0.957
318	558.588	0.932
328	264.911	0.916

The enthalpy and entropy of adsorption, which are determined using the van't Hoff equation, are two other essential thermodynamic factors. The van't Hoff equation is (Equation 5) [18]:

$$\ln K = -\frac{\Delta H_{ads}}{RT} + \frac{\Delta S_{ads}}{R} + \ln \frac{1}{55.5} \quad (5)$$

The enthalpy and entropy of adsorption were calculated by plotting lnK against 1/T (Figure 7). ΔH_{ads} and ΔS_{ads} are calculated and reported in Table 5 using the slope ($-\Delta H_{ads}/R$) and intercept ($\Delta S_{ads}/R + \ln 1/55.5$). The following relationship (Equation 6) is used to calculate the Gibbs free energy for adsorption ΔG_{ads} [19].

$$\Delta G_{ads} = \Delta H_{ads} - T\Delta S_{ads} \ldots \quad (6)$$
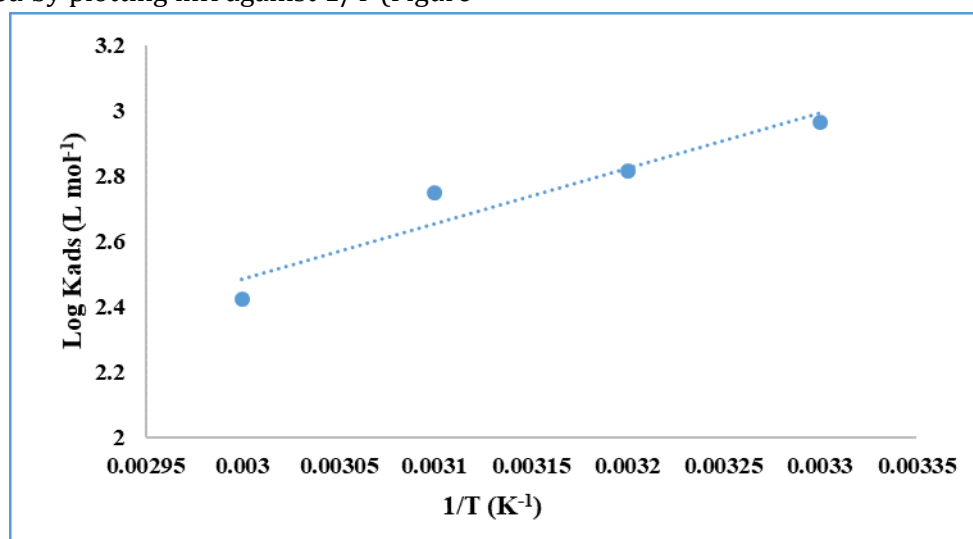
FIGURE 7 Plot of log K_{ads} versus 1/T

TABLE 5 Thermodynamic parameters ΔH_{ads}, ΔS_{ads} and ΔG_{ads} for the adsorption of FATH inhibitor on the carbon steel surface

T (K)	$-\Delta G_{ads}$ (kJ. mol^{-1})	ΔH_{ads} (kJ.mol^{-1})	ΔS_{ads} (kJ.mol^{-1})	R^2
298	26.8743			0.9981
308	29.4275			0.9569
318	27.3382	-32.4946	-0.04993	0.9315
328	30.3333			0.9164

The exothermic nature of the dissolution of carbon steel in hydrochloric acid solution is reflected by the negative sign of the change in enthalpy (ΔH_{ads}). The entropy change (ΔS_{ads}) of FATH inhibitor adsorption on metal surface is negative. This means that when the adsorption process progresses from reactants to a metal adsorbed species reaction complex, the randomness of the process decreases [20,21]. The ΔG_{ads} of the studied inhibitors is more negative, indicating that adsorption of FATH on carbon steel surface is more spontaneous [22].

Conclusion

According to the results of this study, as the concentration of the inhibitor FATH increases, it displays a high efficiency against carbon steel corrosion. Also, the temperature effect suggests that as the temperature rises, the inhibition efficiency diminishes. Another major result that the activation energy (Ea) of inhibited carbon steel is larger than that of uninhibited carbon steel, indicating that inhibition efficiency is temperature dependent. Finally, the exothermic process is shown by the negative value of ΔH_{ads} and ΔS_{ads}.

Acknowledgements

Orcid:

Nbras Hussein Ali: *https://orcid.org/0000-0001-9447-6568*

References

[1] S.N. Popova, B.N. Popov, R.E. White, D. Drazic, *Corrosion*, **1990**, *46*, 1007. [crossref], [Google Scholar] [Publisher]

[2] J.R. Park, D.D. Macdonald, *Corrosion*, **1989**, *45*, 563-571. [crossref], [Google Scholar] [Publisher]

[3] M.E. Belghiti, S. Bouazama, S. Echihi, A. Mahsoune, A. Elmelouky, A. Dafali, K.M. Emran, B. Hammouti, M. Tabyaoui, *Arab. J. Chem.*, **2020**, *13*, 1499–1519. [crossref], [Google Scholar], [Publisher]

[4] O. Fergachi, F. Benhiba, M. Rbaa, R. Touir, M. Ouakki, M. Galai, B. Lakhrissi, H. Oudda, M. Ebn Touhami, *Mater. Res.*, **2018**, *21*, e20171038. [crossref], [Google Scholar], [Publisher]

[5] Y. El Kacimi, M.A. Azaroual, R. Touir, M. Galai, K. Alaoui, M. Sfaira, M. Ebn Touhami, S. Kaya, *Euro-Mediterr J. Environ. Integr.*, **2017**, *2*, 1-11. [crossref], [Google Scholar], [Publisher]

[6] L.S. Ahamed, *J. Glob. Pharma Technol.*, **2018**, *10*, 298-304. [Pdf], [Google Scholar], [Publisher]

[7] A.F.S. Abdul Rahiman, S. Sethumanickam, *Arab. J. Chem.*, **2017**, *10*, S3358–S3366. [crossref], [Google Scholar], [Publisher]

[8] P. Singh, E. E. Ebenso, L. O. Olasunkanmi, I. B. Obot, M. A. Quraishi, *J. Phys. Chem. C*, **2016**, *120*, 3408–3419. [crossref], [Google Scholar], [Publisher]

[9] C. Verma, M.A. Quraishi, L.O. Olasunkanmi, E.E. Ebenso, *RSC Adv.*, **2015**, *5*, 85417–85430. [crossref], [Google Scholar], [Publisher]

[10] G.Y. Elewady, *Int. J. Electrochem. Sci.*, **2008**, *3*, 1149-1161. [Pdf], [Google Scholar], [Publisher]

[11] E.E. Ebenso, *Bull. Electrochem.*, **2003**, *19*, 209-216. [Google Scholar]

[12] J. Haque, Ch. Verma, V. Srivastava, M.A. Quraishi, E.E. Ebenso, *Results Phys.*, **2018**, *9*, 1481–1493. [crossref], [Google Scholar], [Publisher]

[13] J. Sonowal, P.K. Gogoi, *Int. J. Chem.*, **2010**, *2*, 218-225. [Pdf], [Google Scholar], [Publisher]

[14] K. Adardour, O. Kassou, R. Touir, M. Ebn Touhami, H. El Kafsaoui, H. Benzeid, E.M. Essassi, M. Sfaira, *J. Mater. Environ. Sci.*, **2010**, *1*, 129-138. [Pdf], [Google Scholar], [Publisher]

[15] S. Acharya, S.N. Upadhyay, *Trans. Indian Inst. Met.*, **2004**, *57*, 297-306. [Google Scholar]

[16] A. Kadhim, A.K. Al-Okbi, D.M. Jamil, A. Qussay, A.A. Al-Amiery, T.S. Gaaz, A.M.H. Kadhum, A.B. Mohamad, M.H. Nassir, *Results Phys.*, **2017**, *7*, 4013–4019. [crossref], [Google Scholar], [Publisher]

[17] M. Husaini, *Alger J. Eng. Technol.*, **2021**, *04*, 74-80. [crossref], [Google Scholar], [Publisher]

[18] A.Y. Musa, A.A.H. Khadum, A.B. Mohamad, A.R. Daud, S.K. Kamarudin, *Corros. Sci.*, **2009**, *51*, 2393–2399. [crossref], [Google Scholar], [Publisher]

[19] M. Outirite, M. Lagrene, M. Lebrini, M. Traisnel, C. Jama, H. Vezin, F. Bentiss, *Electrochim. Acta.*, **2010**, *55*, 1670–1681. [crossref], [Google Scholar], [Publisher]

SAMI — Eurasian Chemical Communications

[20] M. Bouklah, B. Hammouti, M. Lagrenee, F. Bentiss, *Corros. Sci.*, **2006**, *48*, 2831-2842. [crossref], [Google Scholar], [Publisher]

[21] N.A. Negm, M.F. Zaki, *Colloids Surf., A Physicochem. Eng. Asp.*, **2008**, *322*, 97–102, 2008. [crossref], [Google Scholar], [Publisher]

[22] S.A. Umoren, E.E. Ebenso, *Mater. Chem. Phys.*, **2007**, *106*, 387–393. [crossref], [Google Scholar], [Publisher]